

PHOTONEUTRON CROSS SECTION OF OXYGEN*

K. N. Geller and E. G. Muirhead

Physics Department, University of Pennsylvania, Philadelphia, Pennsylvania

(Received 27 June 1963)

The photodisintegration of O^{16} has been the subject of recent experimental and theoretical investigations.¹⁻⁴ Only recently has satisfactory convergence of results for the oxygen photoneutron cross section become apparent.⁵ This report presents the cross section with considerably improved energy resolution, thus producing an increase in the observed number of resonances existing between the threshold at 15.6 MeV and 23 MeV. By unfolding from the experimental cross section the known resolution function appropriate to the method of cross-section analysis used, a photoneutron cross-section curve is obtained (see Fig. 4). This agrees well with the corresponding photoproton curve for ground-state transitions inferred from $N^{15}(p, \gamma)O^{16}$ data.⁶ In addition, several narrow compound nucleus states are found in the region of the predicted 1^- single-particle resonances.

The $O^{16}(\gamma, n)O^{15}$ yield curve was inferred from the residual radioactivity obtained with a 24-MeV betatron using a precision energy control circuit providing linearity of the energy scale and good stability.⁷ Yield points were taken at 17-keV intervals from threshold to 17.5 MeV and at 34 keV thereafter. Above 17 MeV, the counting statistics were generally better than 0.2%. The relative

photoneutron cross section was obtained using the second difference method with analytical smoothing.⁸ Representative cross-section curves are presented in Figs. 1 and 2 for selected energy ranges and energy resolutions of 68 and 136 keV, respectively. The resolution of the method (see insets, Figs. 1 and 2) is approximately triangular with full width at half-maximum equal to 2 bin widths (ΔE). For each figure, the experimental yield points were taken with energy separation equal to $\frac{1}{2}\Delta E$ and then analyzed in energy intervals of ΔE thus giving two interlaced sets of cross-section points (open and closed circles in Figs. 1 and 2). The good agreement between the alternate sets gives confidence to the structure ascribed to the cross section. The absolute value of the cross section is obtained by normalizing the integrated cross section to 23 MeV at 19 MeV-mb.¹

The smooth curves in each of these figures are obtained by taking a convolution of the second difference resolution function with a linear superposition of single-level Breit-Wigner shapes for the cross section; interference is neglected. The defining parameters for each resonance (position, width, relative height) were chosen so as to produce a minimum χ^2 fit to the experimental data.

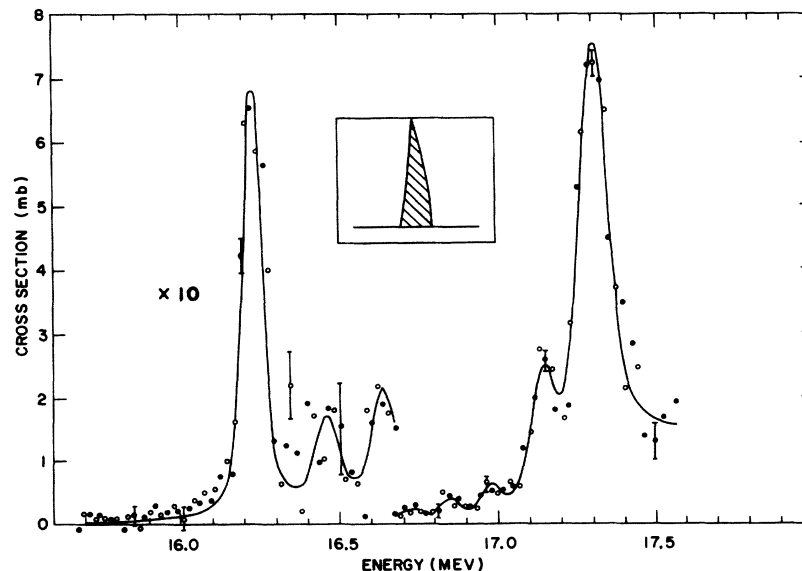


FIG. 1. Cross section for the $O^{16}(\gamma, n)O^{15}$ reaction obtained from the second difference method with analytical smoothing. Analysis bin width, $\Delta E = 34$ keV. Resolution (see inset) $FWHM = 68$ keV.

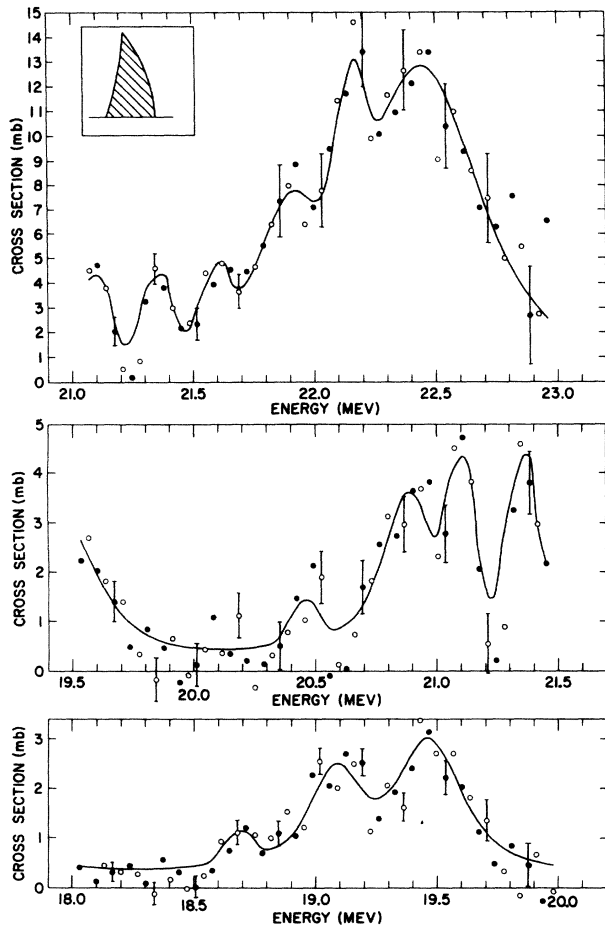


FIG. 2. Cross section for the $O^{16}(\gamma, n)O^{15}$ reaction from 18 to 23 MeV. Analysis bin width, $\Delta E = 68$ keV. Resolution (see inset) $FWHM = 136$ keV.

They are listed in columns 1-3 in Table I. Columns 4-6 present the other level parameters, viz., neutron width (Γ_n), proton width (Γ_p), and radiative width (Γ_γ) deduced from the fits to the empirical data by assuming that the total width is given by the sum of the neutron and proton partial widths, i. e., $\Gamma \approx \Gamma_p + \Gamma_n$. The ratio Γ_p/Γ_n is obtained from available (γ, p) data⁹ and our (γ, n) cross section, each averaged over 0.5-MeV intervals. The radiative width, Γ_γ , is then estimated from the relation

$$\Gamma_\gamma = [4\pi\lambda_\gamma^2 g(J)]^{-1} (1 + \Gamma_p/\Gamma_n) \sigma_0 \Gamma,$$

where the statistical weight factor $g(J) = [(2J+1)/2(2I+1)]$, J^Π is assumed to be 1^- , and I is the spin of the target nucleus, O^{16} . The integrated cross section of each level is given in column 7.

The distribution of dipole strength in the giant

resonance region is shown in Fig. 3. Each radiative width at the corresponding level energy is represented by the height of a vertical line. The two curves show the expected systematic variation of Γ_γ with energy of $E1$ and $M1$ transitions as deduced by Morpurgo¹⁰ from empirical electromagnetic lifetimes of known $E1$ and $M1$ transitions. Also shown in Fig. 3 are the computed values of Elliott and Flowers³ for the radiative width of the O^{16} dipole states in the energy region of this experiment.

The oxygen photoneutron cross section deduced from our experiment with energy resolution unfolded and synthesized by a linear superposition of Breit-Wigner level shapes whose parameters are listed in Table I is shown in Fig. 4. This is compared with the $N^{15}(p, \gamma_0)$ results (dashed curve) of Tanner, Thomas, and Earle⁶ obtained by detailed balancing. The agreement between the gross structure of the two curves is good. The additional fine structure we observe is not at all inconsistent with what one might hope to observe for the actual (γ, n) cross section when the energy resolution is improved. With the notable exception of the region at 19 MeV, satisfactory agreement is also obtained with $O^{16}(\gamma, p)$ cross section⁹ when due allowance is made for the poorer resolution of the latter experiments. An excess (γ, p) cross section which is observed at 19 MeV may be explained as being due to a wrong assignment of specific proton groups to ground-state transitions.

As expected, many of the levels observed in this work have been previously reported in other reactions. The resonance at 16.23 MeV is also observed in the $N^{15}(p, n)$ and $N^{15}(p, \gamma_0)$ reactions. Its calculated Γ_γ of 14 eV is consistent with $M1$ systematics (Fig. 3) and with the $J^\Pi = 1^+$ assignment for this state. There follow five weak resonances in the range 16.4-16.9 MeV whose existence is at the lower level of significance. They may be identified with resonances reported in (p, α) and (p, n) reactions.¹¹ The former reaction populates predominantly $T = 0$ states which are strongly inhibited in photon-induced reactions. Two relatively strong resonances at 17.14 and 17.30 MeV are resolved in the data of Fig. 1, with widths of 45 and 90 keV, respectively; these are in excellent agreement with observations on the $N^{15}(p, n)$ and $N^{15}(p, \gamma_0)$ reactions. An additional broad resonance at 17.55 MeV, $\Gamma = 0.4$ MeV (not shown) is obtained from the analysis with 136-keV resolution. Broad levels have been reported in this energy region for the $N^{15}(p, n)$ reaction

Table I. $O^{16}(\gamma, n)$ level structure.

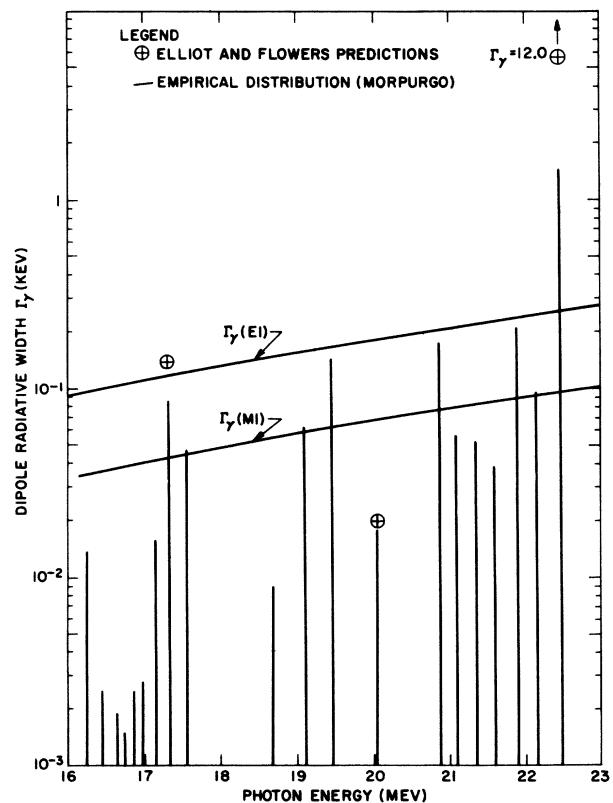
Level energy (MeV) _{lab}	Level width (MeV)	Peak cross section (mb)	Neutron width (MeV)	Proton width (MeV)	Radiative width (dipole) (keV)	Integrated cross section (MeV-mb)
16.23	0.032	1.277	0.004	0.028	0.014	0.064
(16.46)	0.050	0.196	0.007	0.043	0.0025	0.015
(16.63)	0.030	0.294	0.005	0.025	0.0019	0.013
(16.73)	0.020	0.393	0.004	0.016	0.0015	0.012
(16.84)	0.025	0.589	0.006	0.019	0.0025	0.023
(16.97)	0.015	1.228	0.004	0.011	0.0028	0.028
17.14	0.045	2.703	0.014	0.031	0.016	0.190
17.30	0.09	8.355	0.033	0.057	0.086	1.180
17.55	0.40	1.228	0.174	0.226	0.048	0.771
18.68	0.05	1.474	0.021	0.029	0.009	0.115
19.08	0.20	2.211	0.071	0.129	0.063	0.694
19.47	0.30	2.949	0.095	0.205	0.146	1.388
20.45	0.04	2.334	0.012	0.028	0.018	0.146
20.88	0.20	3.563	0.062	0.138	0.138	1.118
21.10	0.025	11.796	0.008	0.017	0.056	0.462
21.35	0.025	11.304	0.009	0.016	0.052	0.443
21.59	0.025	8.847	0.009	0.016	0.039	0.347
21.89	0.25	4.915	0.097	0.153	0.210	1.929
22.15	0.04	13.762	0.016	0.024	0.095	0.864
22.47	0.60	12.779	0.221	0.379	1.457	12.037

having energy and width [hereafter designated $E(\Gamma)$] equal to 17.0(~ 0.2) and 17.5(~ 0.25) MeV. The energy region from 17.6 to 18.6 MeV is apparently devoid of resonant structure, in contrast to the four narrow resonances inferred from "breaks" in photoactivation curves.¹² From 18.4 to 20.0 MeV the cross section is synthesized by three resonances with $E(\Gamma)$ equal to 18.68(0.050), 19.08(0.200), and 19.47(0.300) MeV. The last two levels are observed in the $N^{15}(p, \gamma_0)$ reaction and more recently by Bramblett, Caldwell, and Fultz¹³ in the $O^{16}(\gamma, n)$ reaction using fast positron annihilation gamma rays with 3% energy resolution.

In the region (20.0 to 21.3 MeV) immediately before the giant resonance, our data is fitted by three resonances with $E(\Gamma)$ equal to 20.45(0.040), 20.88(0.200), and 21.10(0.025) MeV. Previously only one broad resonance has been reported in this region at 20.8 MeV.^{6,13}

The giant resonance region (21.3-23.0 MeV) is shown in Fig. 2 with five levels 21.35(0.025),

FIG. 3. Distribution of radiative widths from threshold to 23 MeV for the levels of O^{16} . For comparison the predictions of Elliott and Flowers and the systematic E1 and M1 variations of Morpurgo are included.



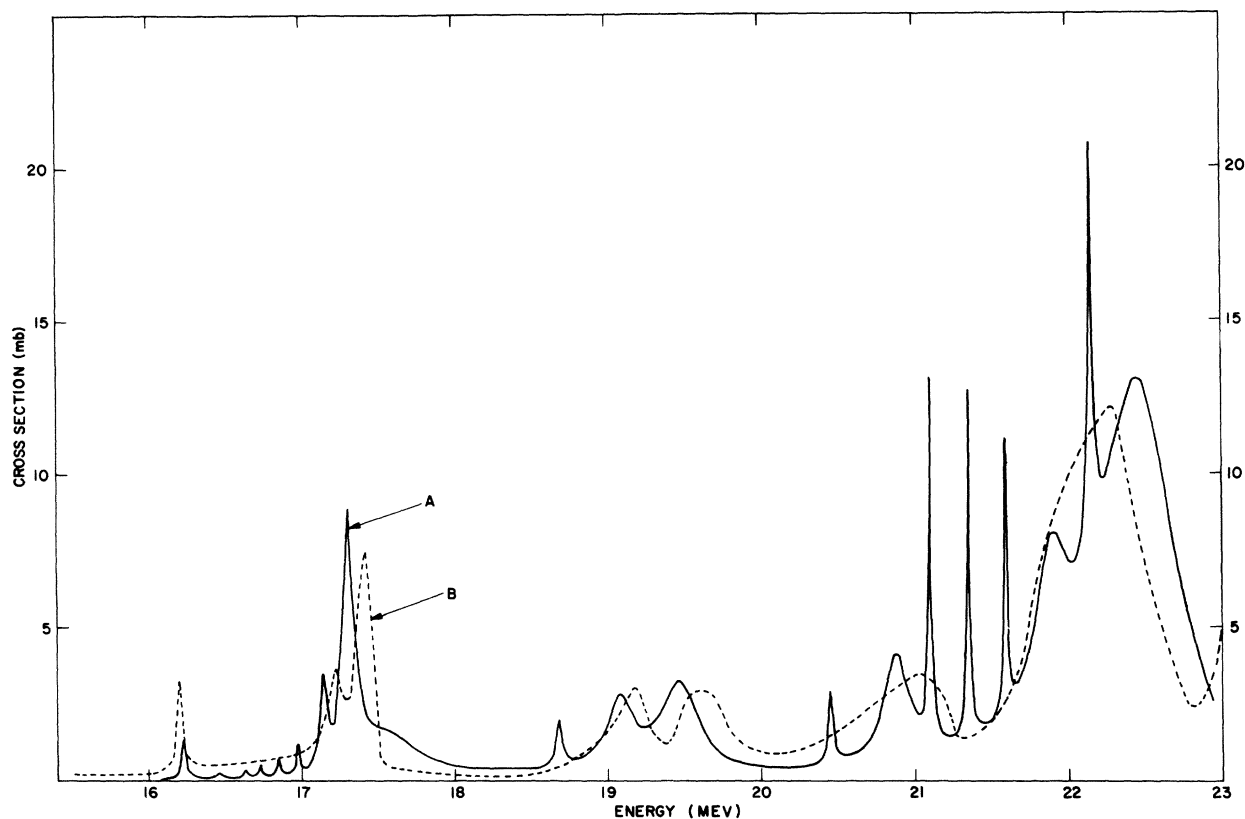


FIG. 4. The cross section for the $O^{16}(\gamma, n)$ reaction with energy resolution unfolded from the data of Table I (curve A). For comparison, the $O^{16}(\gamma, p_0)N^{15}$ cross section, obtained by detailed balancing from the data of reference 6, is shown (curve B).

21.59(0.025), 21.89(0.25), 22.15(0.040), and 22.47(0.60). The $N^{15}(p, \gamma_0)$ result shows only one strong and wide resonance in this region, whereas the Livermore group obtained additional structure at 21.9 MeV.¹³

It is profitable to make a comparison with the detailed shell-model predictions of Elliott and Flowers.³ Of a total of five single-particle transitions which exhaust the dipole sum rule, only three occur in the energy range of this experiment. The comparison is given in Table II. The agreement between experiment and theory is good for the first two dipole states. However, the strong dipole transitions at 22.47 MeV possesses a radiative width which is about a factor of 8 less than the theoretical limit.

Apart from this discrepancy, the agreement (a) between theory and experiment and (b) with the $N^{15}(p, \gamma_0)$ experiment is satisfactory. The additional fine structure observed is accounted for by the improvement in energy resolution in the present experiment. The dipole strength of the single-particle states appears to be shared among com-

pound nuclear states of more highly excited configurations which possess the same symmetry properties of the neighboring single-particle state ($J^{\pi}, T = 1^-, 1$). In this context, it seems reasonable to associate the compound nucleus states at 17.14, 17.305, and 17.55 MeV with the single-particle state at 17.3 MeV. A value of 150 eV is obtained for the sum of the radiative widths of these levels; the single-particle estimate is 140

Table II. Comparison of resonance parameters of calculations of Elliott and Flowers^a with this experiment.

Level configuration	Theoretical		Experimental	
	Energy (MeV)	Radiative Width (Γ_{γ}) (keV)	Energy (MeV)	Radiative Width (Γ_{γ}) (keV)
$p_{1/2}^{-1}d_{3/2}$	17.3	0.140	17.3	0.086
$p_{3/2}^{-1}s_{1/2}$	20.4	0.02	20.45	0.018
$p_{3/2}^{-1}d_{5/2}$	22.6	12.0	22.47	1.46

^aSee reference 3.

eV. This mixing of the single-particle states into one or more compound nucleus state is introduced by the residual nucleon-nucleus interactions. Thus, the clustering of narrow levels in the vicinity of a single-particle state is to be expected.

*Work supported in part by the U. S. Air Research and Development Command, U. S. Office of Naval Research, and the National Science Foundation.

¹L. N. Bolen and W. D. Whitehead, *Phys. Rev. Letters* **9**, 458 (1962).

²F. W. K. Firk and K. H. Lokan, *Phys. Rev. Letters* **8**, 321 (1962); N. A. Burgov, G. R. Danilyan, B. S. Dolbilkin, L. E. Lazareva, and F. A. Nikolaev, *Zh. Eksperim. i Teor. Fiz.* **43**, 70 (1962) [translation: *JETP* **16**, 50 (1963)]; J. Miller, G. Schuhl, G. Tamas, and C. Tzara, *Phys. Letters* **2**, 76 (1962); D. W. Anderson, A. J. Bureau, B. C. Cook, J. E. Griffin, J. R. McConnell, and K. H. Nybo, *Phys. Rev. Letters* **10**, 250 (1963).

³J. P. Elliott and B. H. Flowers, *Proc. Roy. Soc.*

(London) **A242**, 57 (1957).

⁴G. E. Brown, L. Castillejo, and J. A. Evans, *Nucl. Phys.* **22**, 1 (1961).

⁵Evans Hayward, *Rev. Mod. Phys.* **35**, 324 (1963).

⁶N. W. Tanner, G. C. Thomas, and E. D. Earle, *Proceedings of the Rutherford Jubilee International Conference, Manchester, 1961*, edited by J. B. Birks (Heywood and Co., London, 1962).

⁷K. N. Geller, *Nucl. Instr. Methods* **17**, 161 (1962).

⁸K. N. Geller, *Phys. Rev.* **120**, 2147 (1960); K. N. Geller and E. G. Muirhead (to be published).

⁹E. G. Fuller and Evans Hayward, *Nuclear Reactions*, edited by P. M. Endt and P. B. Smith (North-Holland Publishing Company, Amsterdam, 1962), Vol. II.

¹⁰G. Morpurgo, *Proceedings of the International School of Physics "Enrico Fermi," Course XV, 1960*, p. 164 (unpublished).

¹¹F. Ajenberg-Selove and T. Lauritsen, *Nucl. Phys.* **11**, 1 (1959).

¹²A. L. Penfold and B. M. Spicer, *Phys. Rev.* **100**, 1377 (1955).

¹³R. L. Bramblett, J. T. Caldwell, and S. C. Fultz, *Bull. Am. Phys. Soc.* **8**, 120 (1963).

KINETIC ENERGY AND PROMPT NEUTRON DISTRIBUTIONS IN FISSION

Peter Fong*

Physics Department, Utica College of Syracuse University, Utica, New York

(Received 23 August 1963)

Refined experiments in the last few years have established a number of unexpected facts. The kinetic energy of a fission pair as a function of the mass ratio of the two fragments shows a drastic dip in the symmetric fission region.¹ The average number of prompt neutrons per fragment as a function of the fragment mass increases almost linearly with mass up to the symmetric fission region and then suddenly drops to near zero; after this it increases almost linearly again (the so-called saw-tooth structure).² These features are difficult to explain in any theory. The difficulty is particularly serious for the statistical theory because these results are in contradiction to the predictions of this theory as carried out in an earlier article³ (referred to as paper I). The purpose of this note is to point out that the statistical theory is still in a position to explain these phenomena provided that all effects of the nuclear shells are taken into account, not only the effect on nuclear masses considered in paper I but also the effect on nuclear deformability.

When we compare the experimental kinetic energy with the predicted energy curve (essen-

tially due to Coulomb repulsion) in paper I, we notice that the experimental value is consistently higher than the Coulomb energy value in the neighborhood of fragment mass 133 while in the symmetric fission region it is lower. Since the experimental result in the latter region is less accurate than in the former, it is probably wiser to emphasize the abnormal "peak" of the kinetic energy around mass 133 over and above the Coulomb energy curve rather than the dip in the symmetric fission region. This is more so when we recognize that the peaks for isotopes from U^{233} up all fall in the same region where the primary fission fragments are near the 82-neutron shell. The above point of view is further strengthened by the recent work of Britt, Wegner, and Gursky⁴ on the fission of isotopes far below U^{233} , which shows no dip in the symmetric fission region (Bi^{209} , Au^{197} , and Ra^{226}) but also shows the peak in the same mass region as before (Ra^{226}), only far removed from the symmetric fission region (too far to be observed in Bi^{209} and Au^{197}). Similarly, Niday's curve¹ for U^{235} shows the peak and also a flat region in symmetric fission. The prompt-neutron dis-